Torque in magnetospheric star-disk interaction

Miljenko Čemeljić

College of Astronomy and Natural Sciences, SGMK Nicolaus Copernicus Superior School, Warsaw, Poland

&

Institute of Physics, Silesian University in Opava, Czech Republic

&

Nicolaus Copernicus Astronomical Center, PAN Warsaw, Poland

&

Academia Sinica Institute of Astronomy and Astrophysics, Taipei, Taiwan

Outline

- Introduction
- Analytical thin HD disk solution
- Numerical simulations in HD and MHD
- “Atlas” of solutions
- Trends in the angular momentum flux
- Addition of the magnetic field inside the disk
- Summary

Introduction

•First numerical solution of (HD) accretion disk was by Prendergast & Burbidge (1968)

•Analytical solution was given by Shakura & Sunyaev (1973)

• … (lots of good things, but mostly with 1D, vertically averaged models)

•In Kita (1995, PhD Thesis) and Kluźniak & Kita (2000, KK00) was given a solution of the thin HD polytropic disk in the full 3D. It was obtained by the method of asymptotic approximation with the disk thickness as a small parameter.

•In 2009, numerical simulations of star-disk magnetospheric interaction were done in 2D-axisymmetric simulations, by Romanova et al. (2009, 2013, with non-public code), Zanni & Ferreira (2009, 2013, with the publicly available PLUTO code).

•In Čemeljić (2019), A&A, 624, A31, I repeated the Zanni et al. (2009, 2013) 2D axisymmetric viscous & resistive MHD simulations with PLUTO (ver. 4.1), and went on to a parameter study, to investigate the trends in dependence of different parameters (Čemeljić & Brun, 2023) and directly compare the solutions with analytical computations (Čemeljić, Kluźniak & Parthasarathy, 2023). In our group in Warsaw, we also investigated simulations with meridional backflow (Mishra, Čemeljić & Kluźniak, 2023), axial outflows (Kotek et al, 2020) and other than stellar dipole magnetic field (Cieciuch & Čemeljić, 2022).

Kluźniak-Kita thin disk analytical solutions

Initial conditions are HD disk and a hydrostatic corona. Examples from derivation:

Equation of continuity:

$$\frac{\epsilon}{r}\frac{\partial}{\partial r}\left(r\rho v_r\right)+\frac{\partial}{\partial z}\left(\rho v_z\right)=0 \tag{1}$$

Order ϵ^0:

$$\frac{\partial}{\partial z}\left(\rho_0 v_{z0}\right)=0 \;\Rightarrow v_{z0}=0 \tag{2}$$

Order ϵ^1:

$$\frac{1}{r}\frac{\partial}{\partial r}\left(r\rho_0 v_{r0}\right)+\frac{\partial}{\partial z}\left(\rho_0 v_{z1}\right)=0 \tag{3}$$

From the argumentation presented below, for the first order in ϵ of the radial momentum, we have $v_{r0}=0$, so that here we have $\partial_z(\rho_0 v_{z1})=0 \Rightarrow \rho_0 v_{z1}=const$ along z. Since v_z is odd with respect to z, at the disk equatorial plane it is $\rho_0 v_{z1}=0$. Since it does not depend on z, and $\rho_0\neq 0$, we conclude that $v_{z1}=0$.

Order ϵ^2:

$$\frac{1}{r}\frac{\partial}{\partial r}\left(r\rho_0 v_{r1}\right)+\frac{\partial}{\partial z}\left(\rho_0 v_{z2}\right)=0 \tag{4}$$

Vertical momentum:

$$\begin{aligned}\epsilon v_r\frac{\partial v_z}{\partial r}+v_z\frac{\partial v_z}{\partial z}=&-\frac{z}{r^3}\left[1+\epsilon^2\left(\frac{z}{r}\right)^2\right]^{-3/2}\\ -n\frac{\partial c_s^2}{\partial z}&+\frac{2}{\gamma\tilde{\beta}}\frac{1}{\rho}\left(\epsilon B_r\frac{\partial B_z}{\partial r}+B_z\frac{\partial B_z}{\partial z}\right)-\frac{1}{\gamma\tilde{\beta}}\frac{1}{\rho}\frac{\partial B^2}{\partial z}\\ &+\frac{2}{\rho}\frac{\partial}{\partial z}\left(\eta\frac{\partial v_z}{\partial z}\right)+\frac{\epsilon^2}{\rho r}\frac{\partial}{\partial r}\left(r\eta\frac{\partial v_z}{\partial r}\right)\\ &-\frac{2}{3}\frac{\epsilon}{\rho}\frac{\partial}{\partial z}\left(\frac{\eta}{r}\frac{\partial}{\partial r}\left(rv_r\right)\right)-\frac{2}{3\rho}\frac{\partial}{\partial z}\left(\eta\frac{\partial v_z}{\partial z}\right)\\ &+\frac{\epsilon}{\rho r}\frac{\partial}{\partial r}\left(\eta r\frac{\partial v_r}{\partial z}\right)\end{aligned} \tag{17}$$

Order ϵ^0:

$$0=-\frac{z}{r^3}-n\frac{\partial c_{s_0}^2}{\partial z}-\frac{1}{\gamma\tilde{\beta}}\frac{1}{\rho_0}\frac{\partial B_0^2}{\partial z} \tag{18}$$

Since we had $\partial B_{r0}/\partial z=\partial B_{z0}/\partial z=\partial B_{\varphi 0}/\partial z=0$, we have $\partial B_0/\partial z=0$, i.e. $B_0=f(r)$. We have then

$$\frac{z}{r^3}=-n\frac{\partial c_{s_0}^2}{\partial z}, \tag{19}$$

which is the vertical hydrostatic equilibrium equation, with the solution in the case of $n=3/2$:

$$c_{s0}=\sqrt{\frac{h^2-z^2}{3r^3}},\;\rho_0=\left(\frac{h^2-z^2}{5r^3}\right)^{3/2}, \tag{20}$$

where h is the semi-thickness of the disk. This also gives us the pressure relation $P=\rho_0^{5/3}=[(h^2-z^2)/5r^3]^{5/2}$ (Hoshi 1977; Kluźniak & Kita 2000).

Numerical setup

•I perform simulations of a rotating thin Kluźniak-Kita accretion disk, which reach a quasi-stationary state.

•Ohmic and viscous heating in the energy equation are extracted, assuming that all the heat is radiated away.

•Viscosity and resistivity are still included, in the equation of motion and in the induction equation.

$$\frac{\partial \rho}{\partial t} + \nabla \cdot (\rho \boldsymbol{u}) = 0$$

$$\frac{\partial \rho \boldsymbol{u}}{\partial t} + \nabla \cdot \left[\rho \boldsymbol{u}\boldsymbol{u} + \left(P + \frac{\boldsymbol{B} \cdot \boldsymbol{B}}{8\pi} \right) \boldsymbol{I} - \frac{\boldsymbol{B}\boldsymbol{B}}{4\pi} - \boldsymbol{\tau} \right] = \rho \boldsymbol{g}$$

$$\frac{\partial E}{\partial t} + \nabla \cdot \left[\left(E + P + \frac{\boldsymbol{B} \cdot \boldsymbol{B}}{8\pi} \right) \boldsymbol{u} - \frac{(\boldsymbol{u} \cdot \boldsymbol{B})\, \boldsymbol{B}}{4\pi} \right]$$
$$+ \nabla \cdot [\eta_{\mathrm{m}} \boldsymbol{J} \times \boldsymbol{B}/4\pi - \boldsymbol{u} \cdot \boldsymbol{\tau}] = \rho \boldsymbol{g} \cdot \boldsymbol{u} - \Lambda_{\mathrm{cool}}$$

$$\frac{\partial \boldsymbol{B}}{\partial t} + \nabla \times (\boldsymbol{B} \times \boldsymbol{u} + \eta_{\mathrm{m}} \boldsymbol{J}) = 0.$$

•Code used is PLUTO (v.4.1) by Mignone et al. (2007).

Star-disk simulations with magnetic field

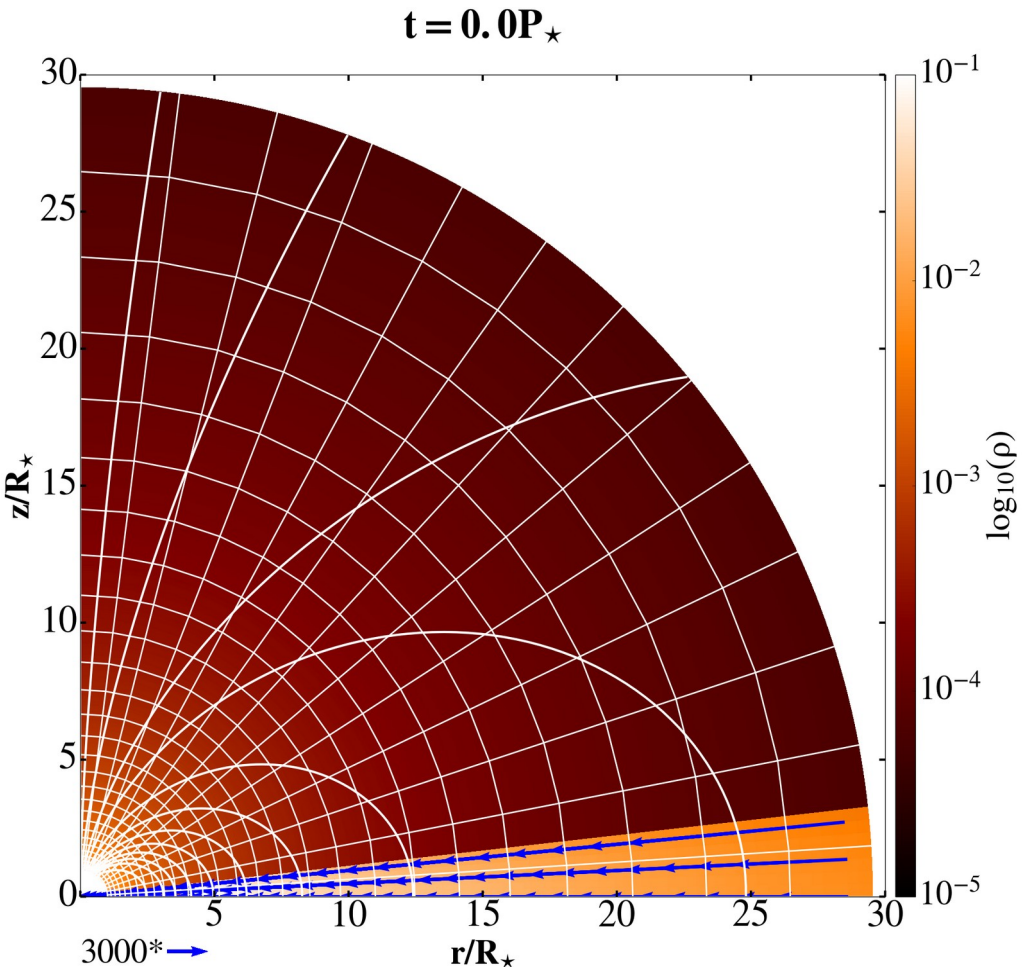

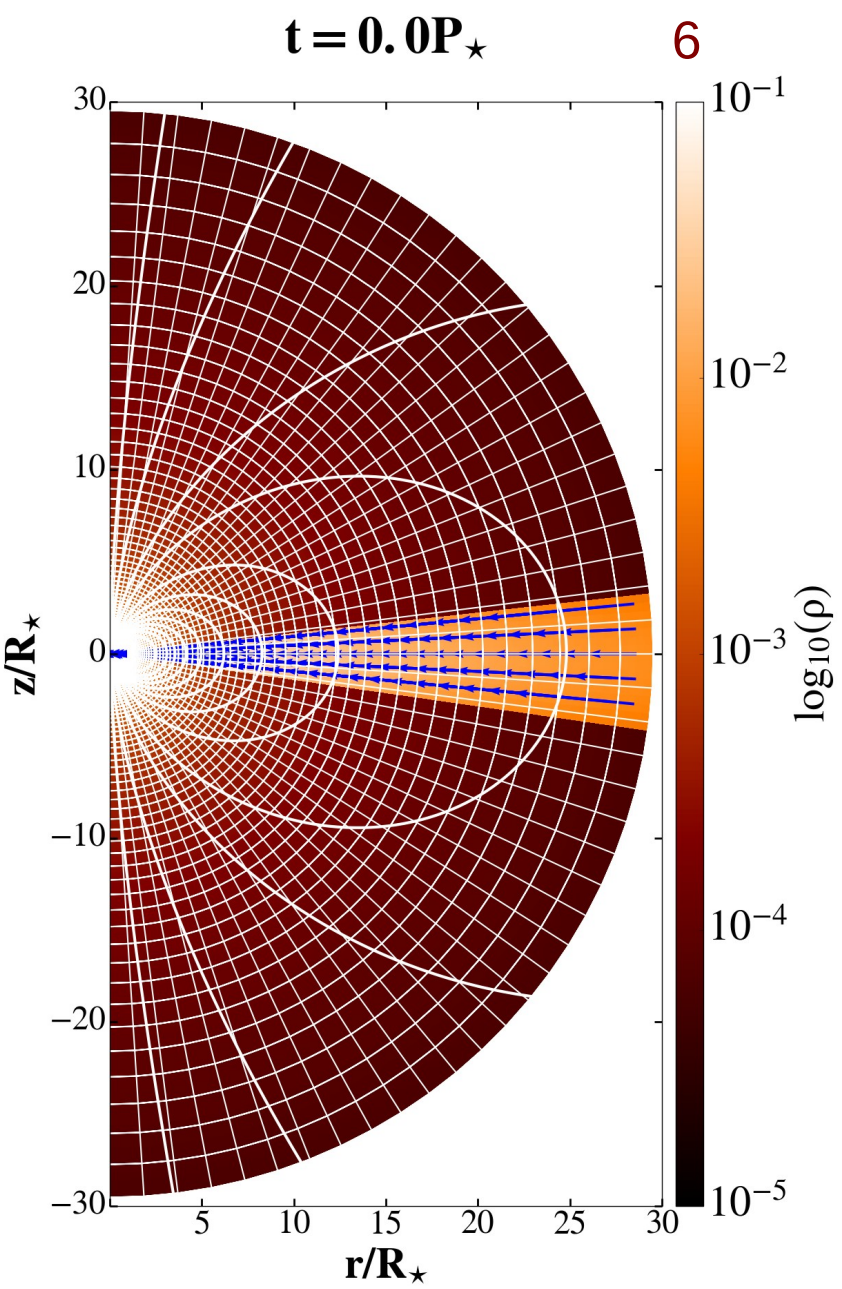

- First we perform purely HD simulations and then we add the magnetic field to the HD solution.
- We assume the star to be a magnetized rotator. Stellar surface is a rotating boundary condition at the origin of the spherical computational domain. The initially non-rotating corona is in a hydrostatic balance, which soon corotates with the disk.

Hydro-dynamic star-disk analytical solutions and simulations[7]

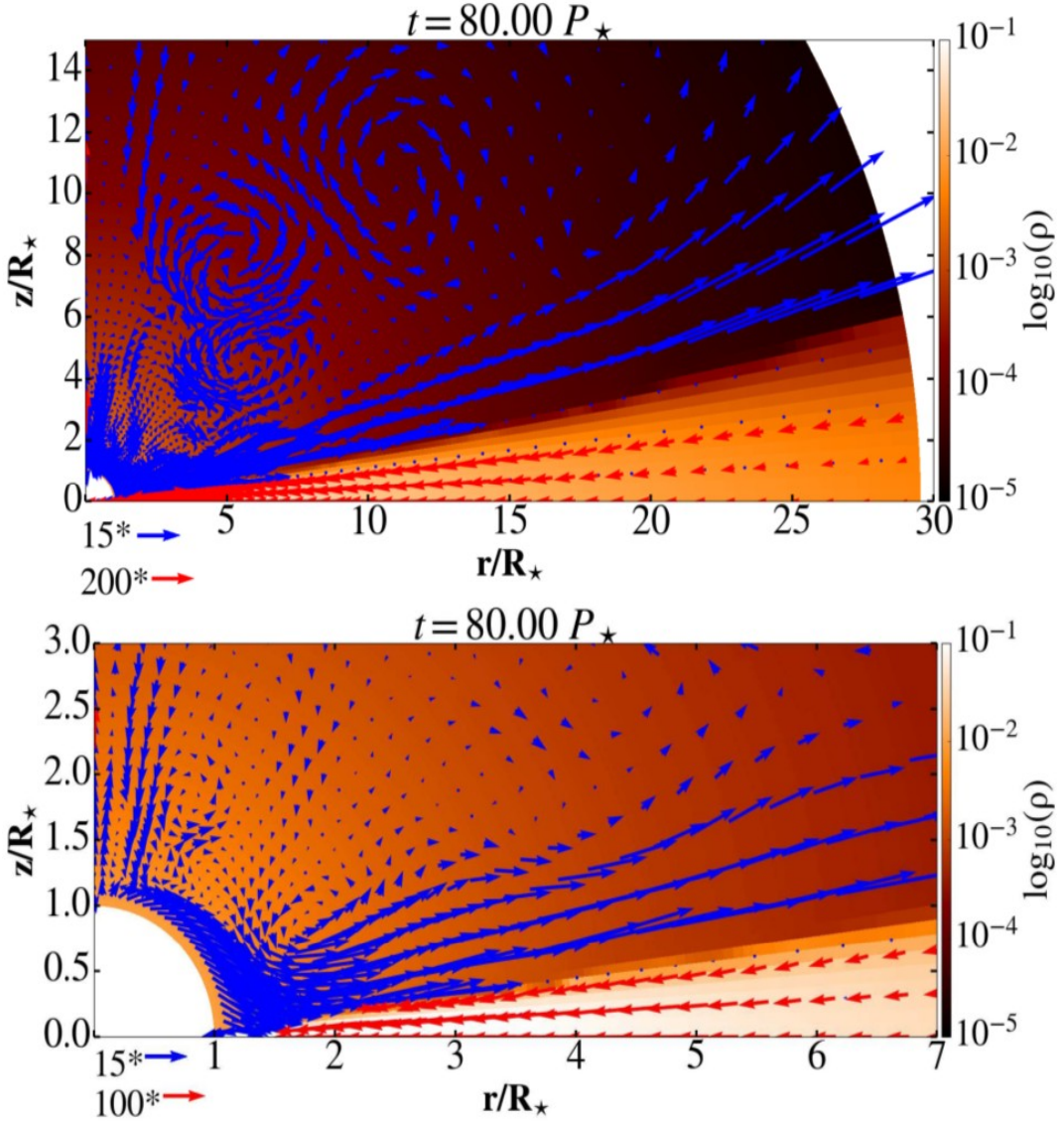

Computational box and a zoom closer to the star after 80 stellar rotations. In color is shown the density, and vectors show velocity, with the different normalization in the disk and stellar wind.

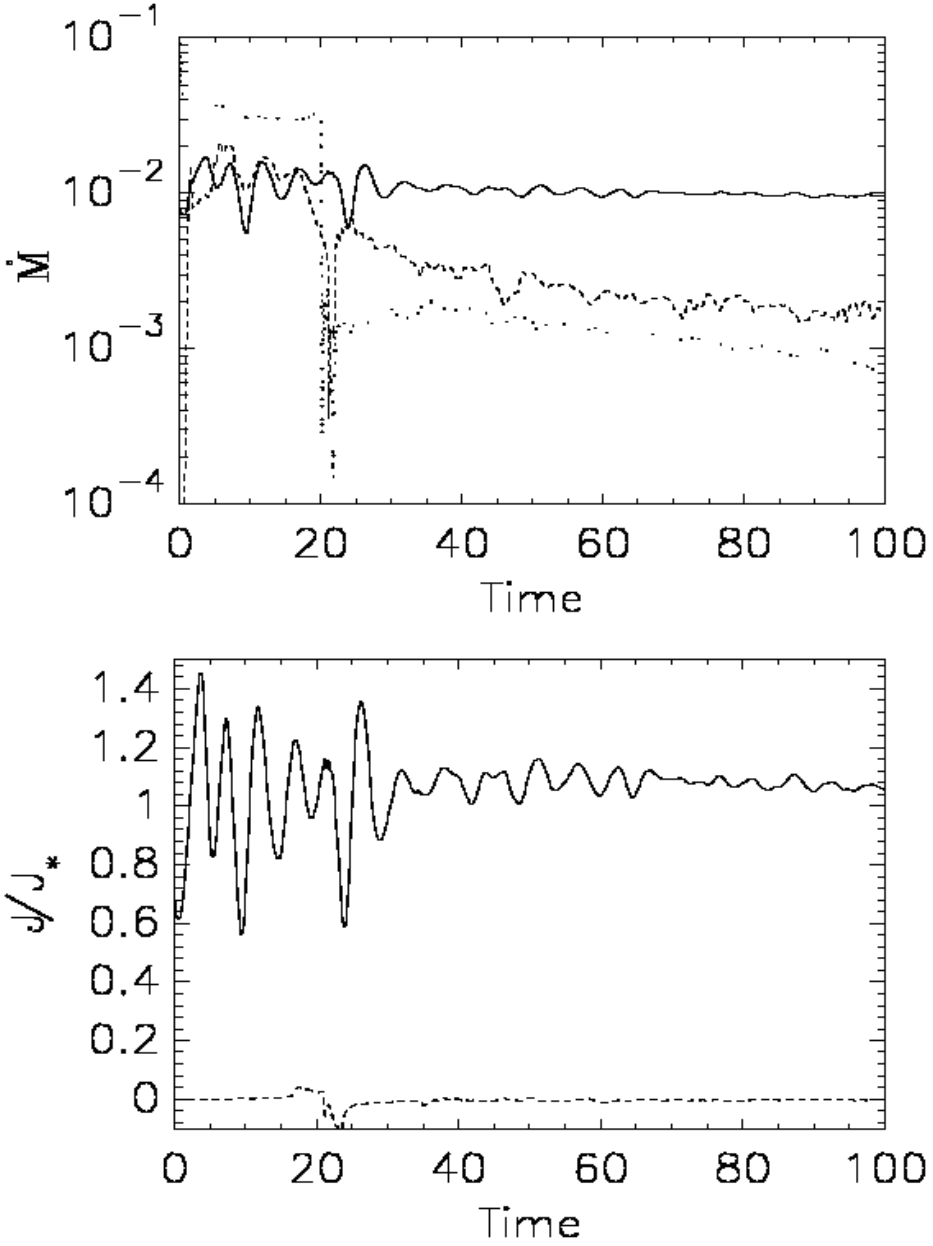

Time dependence of the mass and angular momentum fluxes in the various components in our simulations.

Star-disk simulations $\alpha_v=1.$

Table 1. The parameters in our study presented in the "Atlas": the stellar angular velocity $\Omega_\star$, stellar dipole magnetic field strength $B_\star$, and the magnetic Prandtl number P_m-for which we also table the values of corresponding resistivity coefficient α_m. We show also the stellar rotation period, and corotation radius in young stellar object (YSO) cases.

$\Omega_\star/\Omega_\mathrm{br}$	$B_\star$(G)	P_m	α_m	$P_\star$(days)	$R_\mathrm{cor}(R_\star)$
0.05	250	6.7	0.1	9.2	7.37
0.1	500	1.67	0.4	4.6	4.64
0.15	750	0.95	0.7	3.1	3.54
0.2	1000	0.67	1.0	2.3	2.92

- Prandtl magnetic number:

$$P_\mathrm{m} = \frac{2}{3}\frac{\alpha_\mathrm{v}}{\alpha_\mathrm{m}}$$

Star-disk simulations parameter space

Table 1. We performed 64 star-disk magnetospheric interaction simulations in a setup detailed in Čemeljić (2019). There are all together 64 runs with all the combinations of parameters as listed in the table. The magnetic Prandtl number $P_m = \frac{2}{3}\alpha_v/\alpha_m$ is also listed – in all the cases the anomalous viscosity parameter is $\alpha_v = 1$. The four simulations shown in Fig. 1 are highlighted with boxed bold letters.

$\alpha_m =$	0.1	0.4	0.7	1
$P_m =$	6.7	1.67	0.95	0.67
$\Omega_\star/\Omega_{br}$				
	$B_\star$=250 G			
0.05	a1	a2	a3	a4
0.1	a5	a6	a7	a8
0.15	a9	a10	a11	a12
0.2	a13	a14	a15	a16
	$B_\star$=500 G			
0.05	b1	b2	b3	b4
0.1	**b5**	b6	b7	**b8**
0.15	b9	b10	b11	b12
0.2	b13	b14	b15	b16
	$B_\star$=750 G			
0.05	c1	c2	c3	c4
0.1	c5	c6	c7	c8
0.15	**c9**	c10	c11	c12
0.2	c13	c14	c15	c16
	$B_\star$=1000 G			
0.05	d1	d2	d3	d4
0.1	d5	d6	d7	d8
0.15	d9	d10	d11	**d12**
0.2	d13	d14	d15	d16

I did a systematic study with magnetic star-disk numerical simulations in 64 points in parameter space, for a slowly rotating star.

With PhD students and with summer students, we continued this work, to go to the other parts of the parameter space and other geometries of magnetic field.

The work in full 3D is under way, but 2D axisymmetric results are needed for a comparison with theoretical predictions.

Star-disk magnetospheric interaction (SDMI) simulations

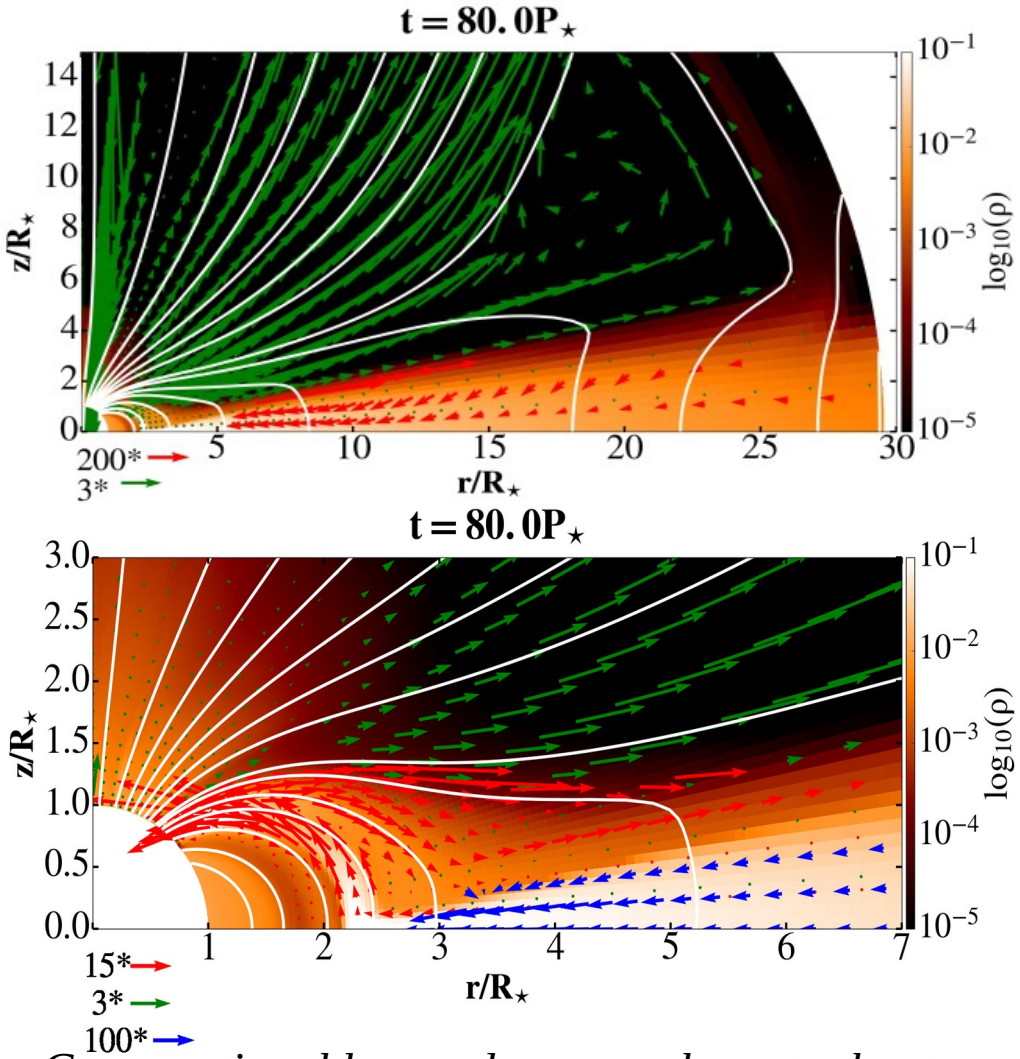

Computational box and a zoom closer to the star after 80 stellar rotations, to visualize the accretion column and the magnetic field lines (white solid lines), connected to the disk beyond the corotation radius Rcor=2.92 Rs. In color is shown the density, and vectors show velocity, with the different normalization in the disk, column and stellar wind.

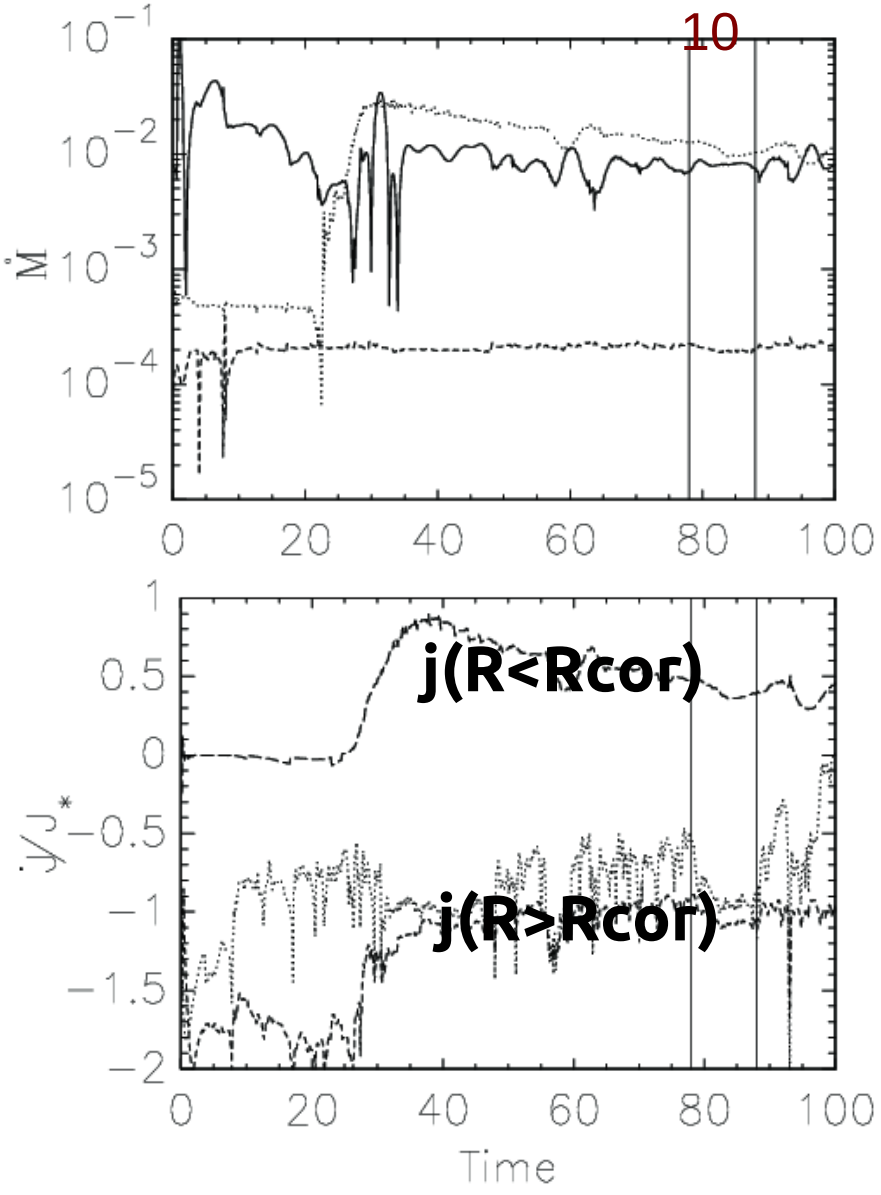

Time dependence of the mass and angular momentum fluxes in the various components in our simulations with marked the time interval in which the average for the quasi-stationarity is computed.

Part of the “Atlas” of solutions for 250 Gauss

Atlas2: Results for density (top panels) and poloidal momentum (bottom panels) in PLUTO simulations of star-disk magnetospheric interactions in different points in the parameter space. Collaborations with Ruchi Mishra (NCAC) and Aleksandra Kotek (Uni Warsaw, NCAC). MČ, April 2020.

$alpha_v$	0.2	0.2	0.2	0.2	0.4	0.4	0.4	0.4	1	1	1	1
$alpha_m$	0.1	0.4	0.7	1	0.1	0.4	0.7	1	0.1	0.4	0.7	1
Pm	1.33	0.33	0.19	0.13	2.67	0.67	0.38	0.63	6.67	1.67	0.95	0.67
B_*=250 Gauss												
$Omega_*$												
0.05									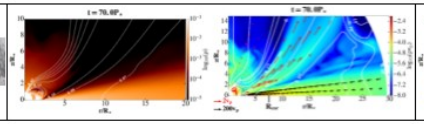	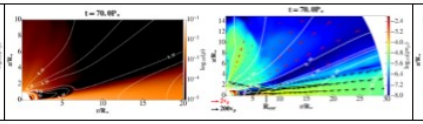	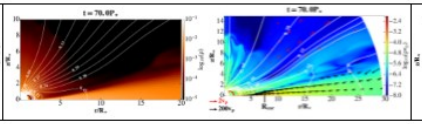	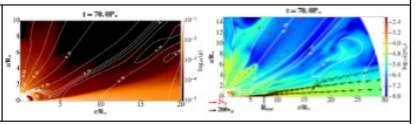
0.1									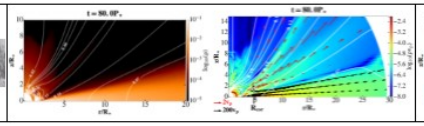	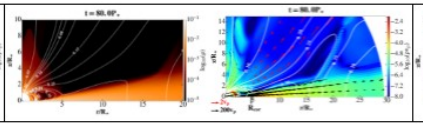	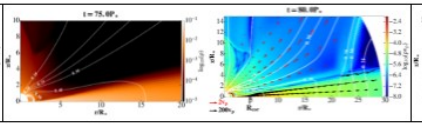	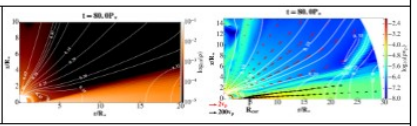
0.15									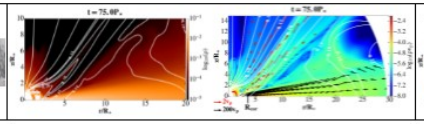	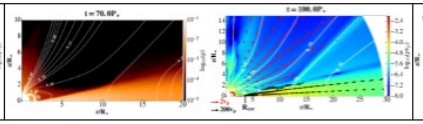	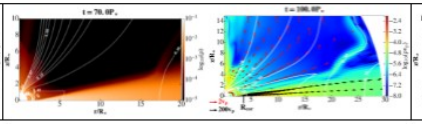	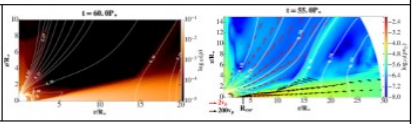
0.2									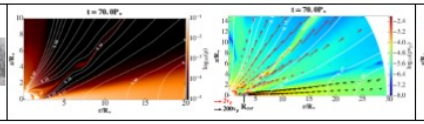	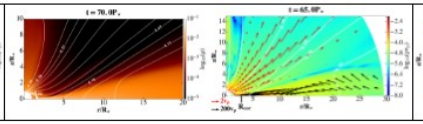	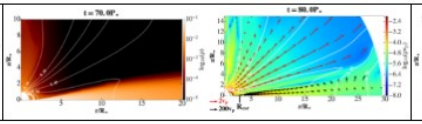	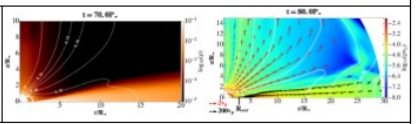
0.4												
0.6												

Example of a solution with 500 Gauss

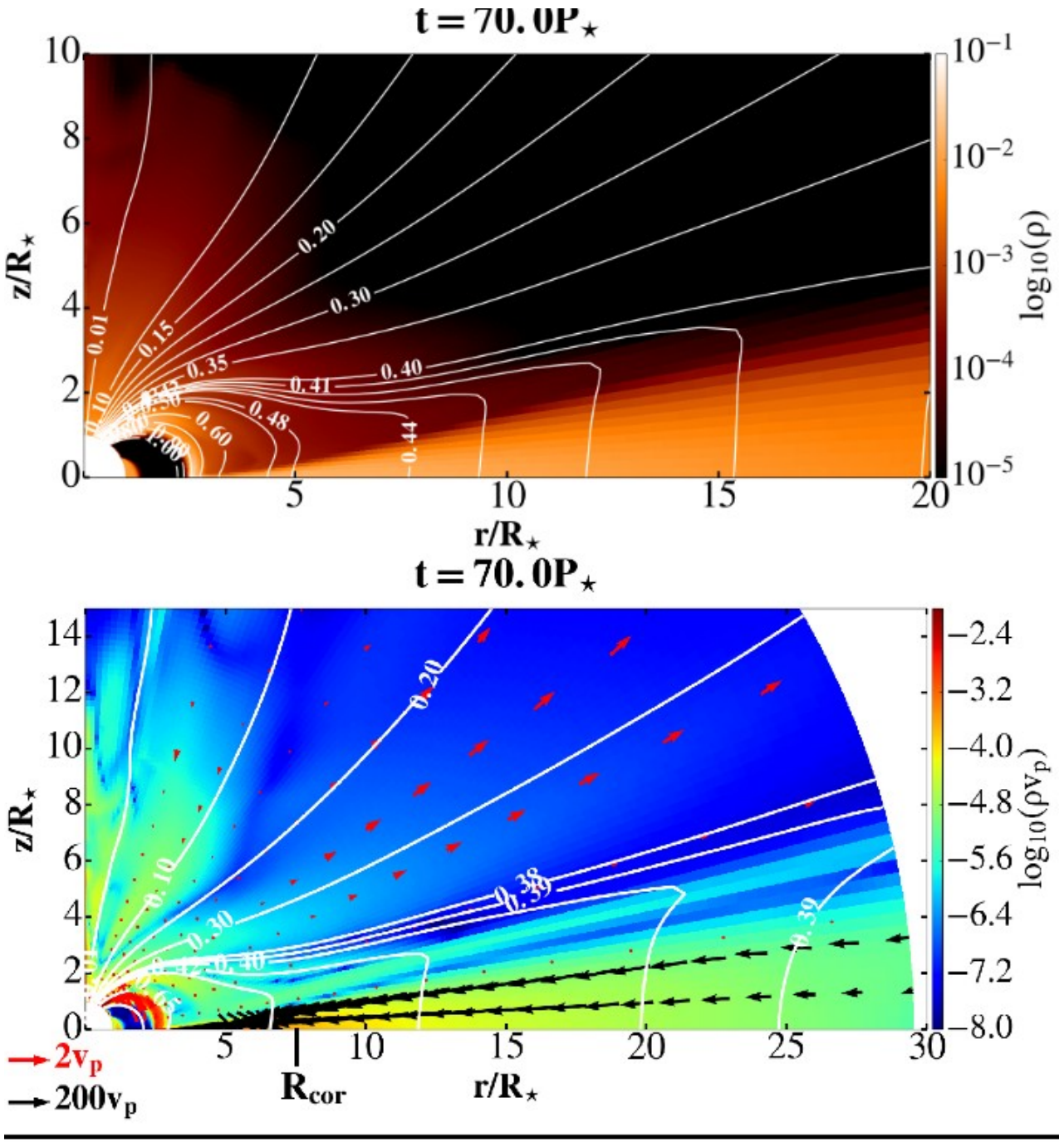

Further analysis of "Atlas" solutions

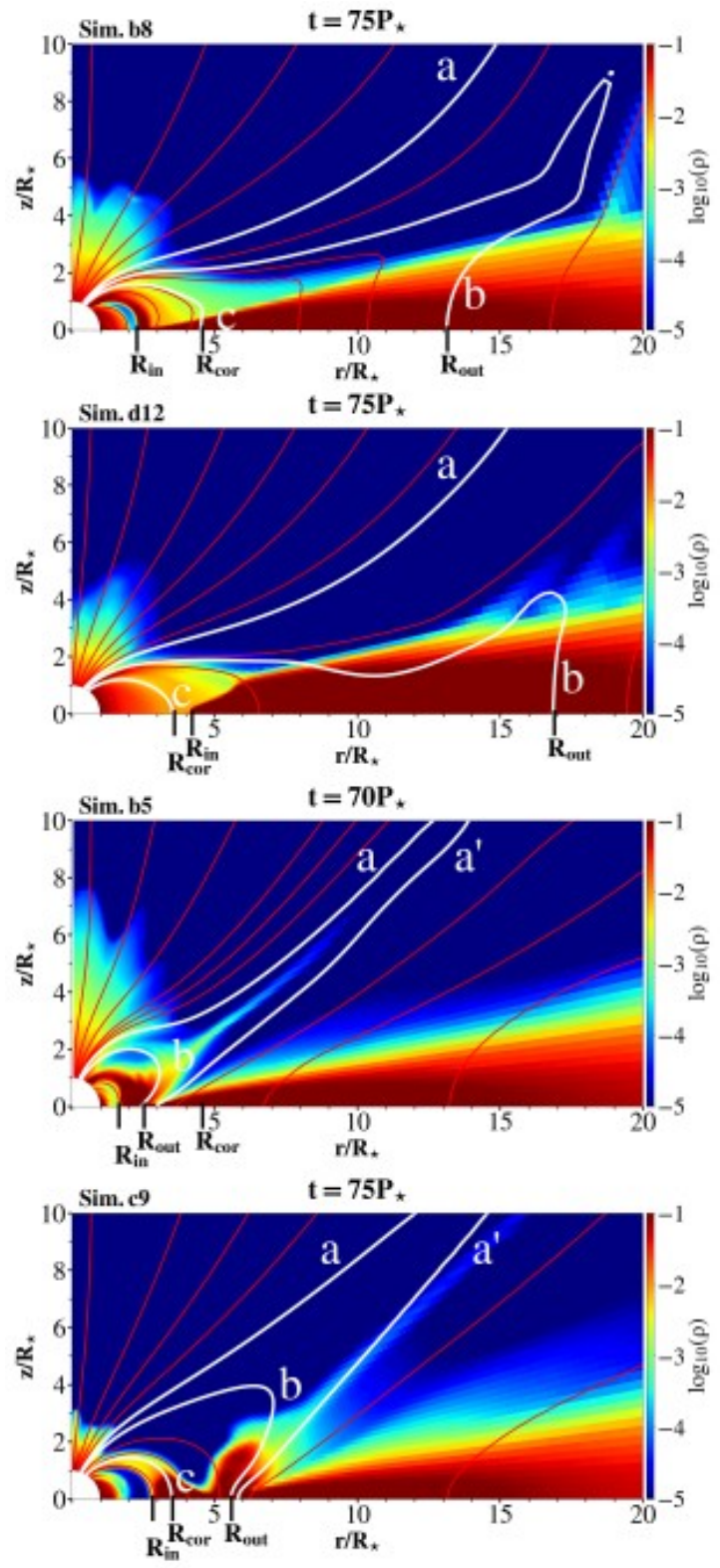

Table 1. 64 star-disk magnetospheric interaction simulations in a setup detailed in Čemeljić (2019).

α_m =	0.1	0.4	0.7	1
P_m =	6.7	1.67	0.95	0.67
$\Omega_\star/\Omega_{br}$				
		$B_\star$ = 250 G		
0.05	**a1**(DCE1)	**a2**(DC)	**a3**(DC)	**a4**(DC)
0.1	**a5**(DCE1)	**a6**(DC)	a7(DC)	**a8**(DC)
0.15	**a9**(DCE1)	**a10**(DC)	a11(DC)	**a12**(DC)
0.2	a13(DCE1)	a14(DC)	a15(DC)	a16(DC)
		$B_\star$ = 500 G		
0.05	**b1**(DCE1)	**b2**(DC)	**b3**(DC)	**b4**(DC)
0.1	**b5** (DCE1)	b6(DC)	b7(DC)	b8 (DC)
0.15	**b9**(DCE1)	b10(DC)	b11(DC)	b12(DC)
0.2	b13(DCE1)	b14(DC)	b15(DC)	b16(DC)
		$B_\star$ = 750 G		
0.05	**c1**(DCE1)	c2(DC)	**c3**(DC)	c4(DC)
0.1	**c5**(DCE1)	c6(DC)	c7(DC)	c8(DC)
0.15	c9 (DCE2)	c10(DC)	c11(DC)	c12(DC)
0.2	c13(DCE2)	c14(DC)	c15(DC)	c16(DC)
		$B_\star$ = 1000 G		
0.05	**d1**(DCE1)	d2(DC)	**d3**(DC)	d4(DC)
0.1	**d5**(DCE1)	d6(DC)	d7(DC)	d8(DC)
0.15	d9(DCE2)	d10(D)	d11(D)	d12 (D)
0.2	d13(DCE2)	d14(D)	d15(D)	d16(D)

If we consider the position of Rcor in the case with conical outflow, there are 4 different cases of solutions. In general, faster stellar rotation prevents the accretion column formation. In the bottom panels resistivity α_m=0.1 and Ω_s=0.1, where a conical outflow is formed, Cemeljic&Brun, (2023).

Comparison of SDMI simulations with increasing mag. field

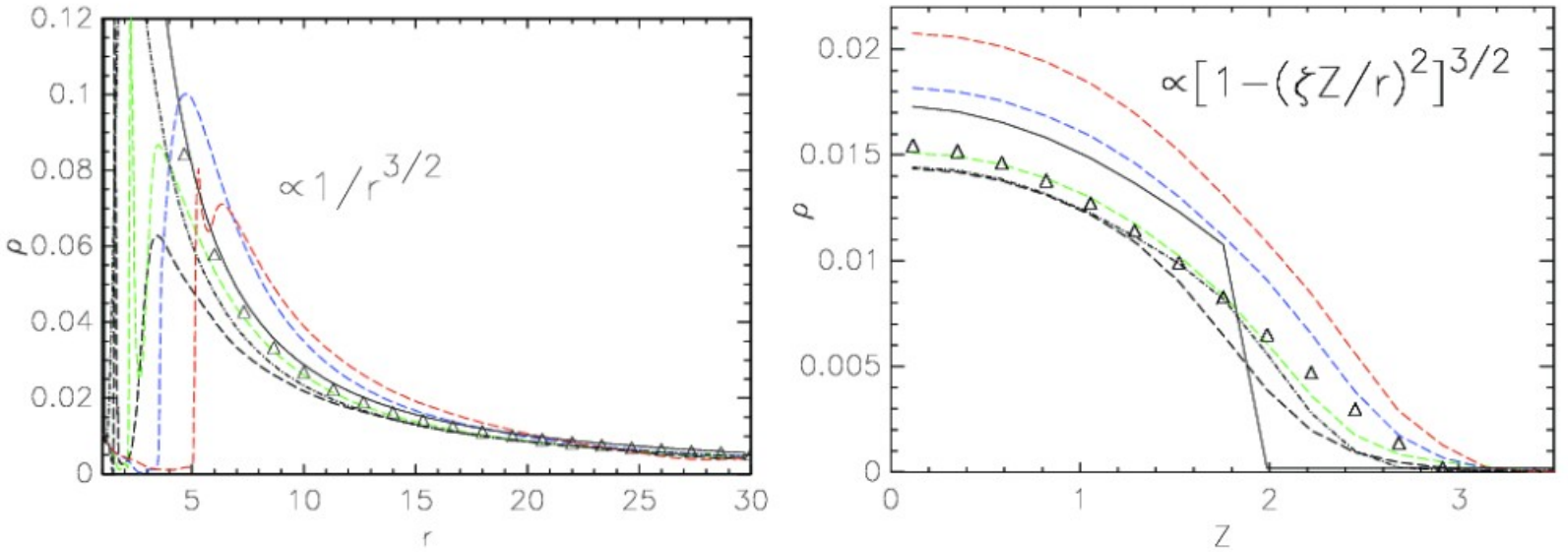

Fig. 3. Comparison of the matter density *Left panel:* radial dependence along the midplane, just above θ=90°. *Right panel:* the profiles along the vertical line at r=15$R_\star$. The legend is the same as in Fig. 2.

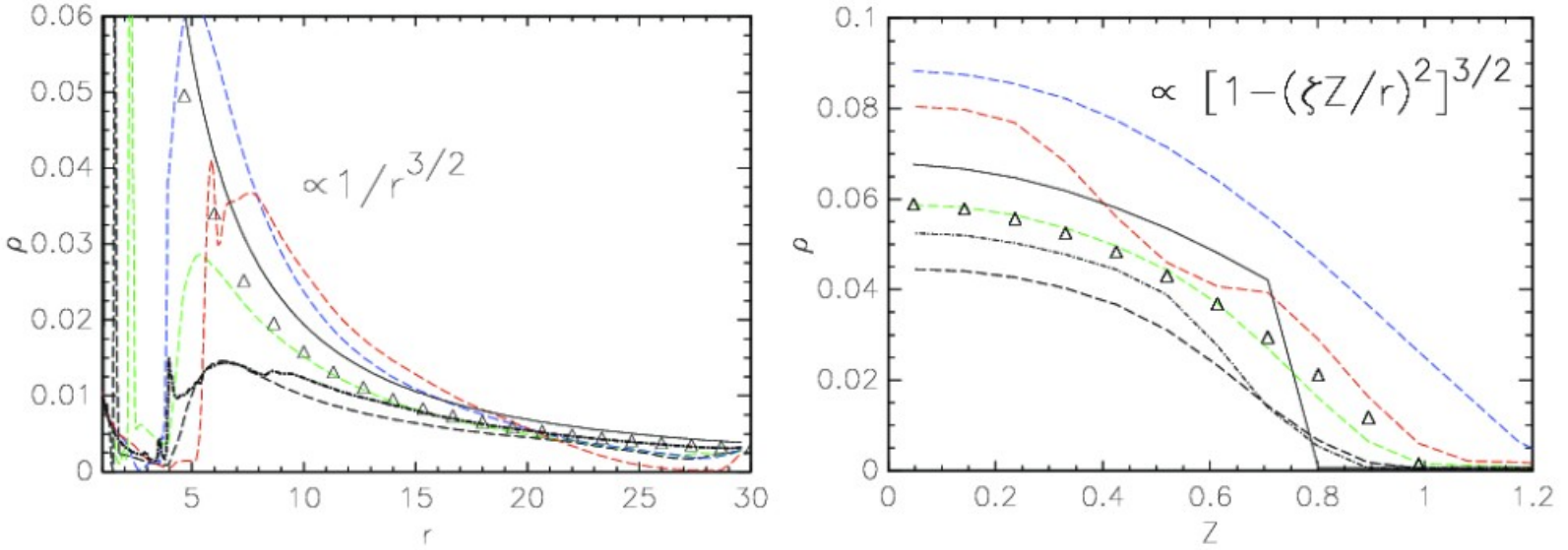

Fig. 4. Comparison of the matter density in the initial set-up (solid line) with the quasi-stationary solutions in numerical simulations in the HD (dot-dashed line) and the MHD cases. *Left panel:* along the disc surface at θ=83°. *Right panel:* along a vertical line at r=6$R_\star$. The meaning of the lines is the same as in Fig. 3.

Comparison of SDMI simulations with increasing mag. field

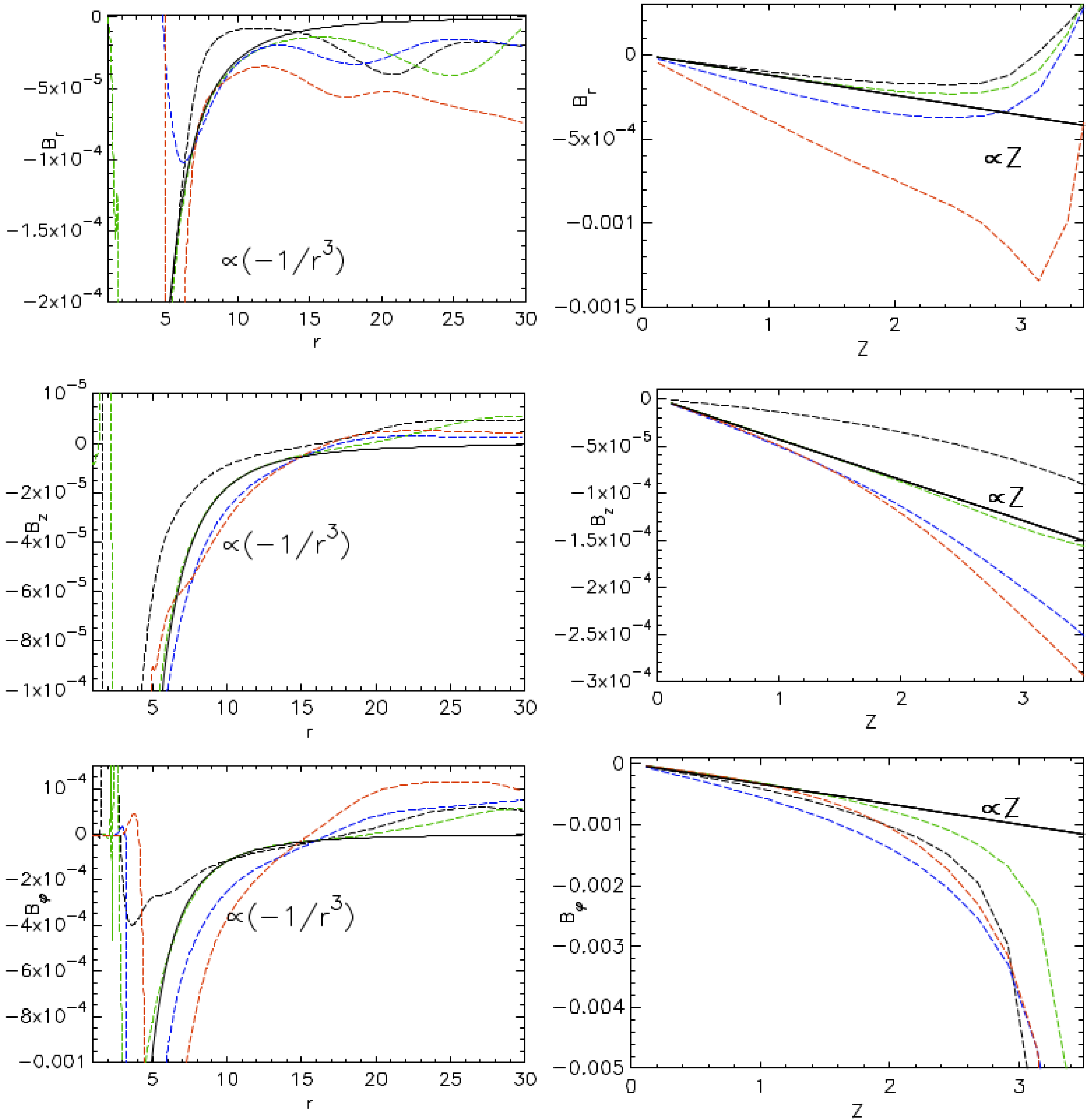

Comparison for magnetic field. In black, green blue and red colors are the results in the MHD cases with the stellar magnetic field strength 0.25, 0.5, 0.75 and 1.0 kG, respectively.

The closest fit to the 0.5 kG case is depicted with the thick solid line.

Trends in angular momentum with increasing stellar magnetic field

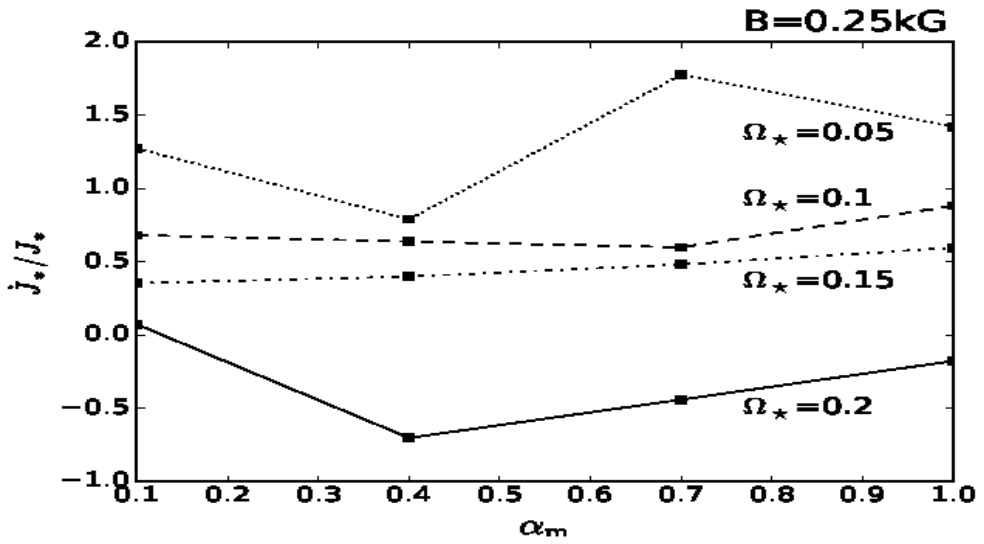

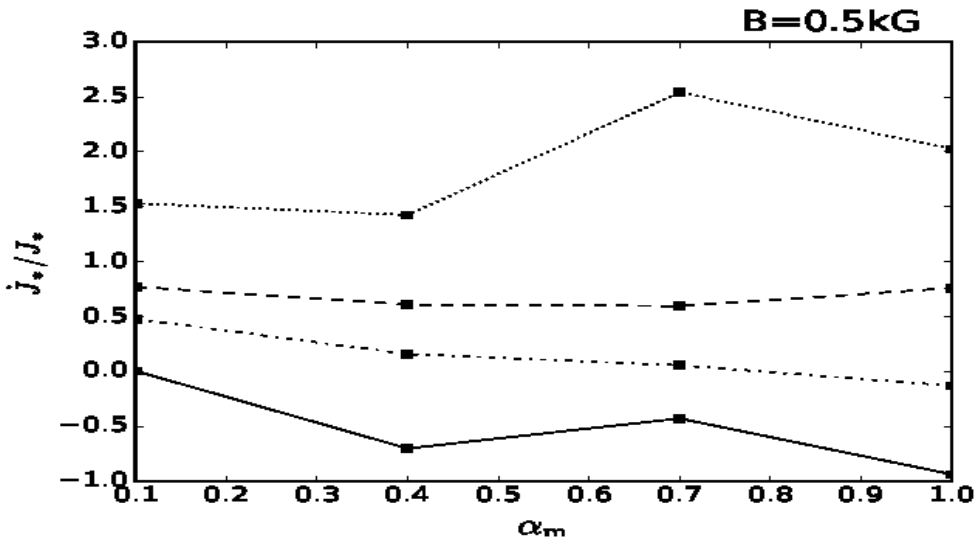

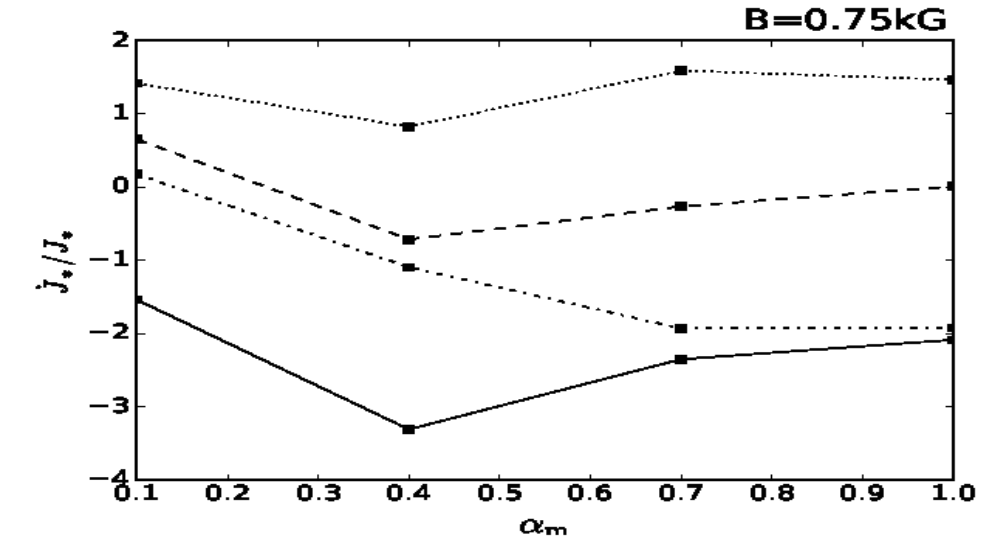

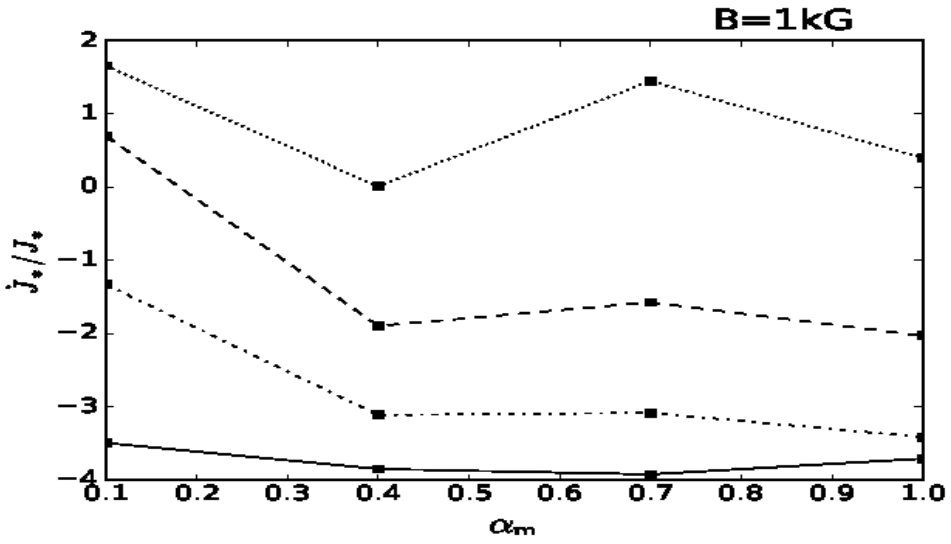

Average angular momentum flux transported onto the stellar surface by the matter in-falling from the disk onto the star through the accretion column. In each panel is shown a set of solutions with one stellar magnetic field strength, varying the stellar rotation rate and resistivity. Positive flux spins-up the star, negative slows it down. With the increase in stellar rotation rate, spin-up of the star by the infalling matter decreases, eventually switching to the spin-down.c

Trends in angular momentum

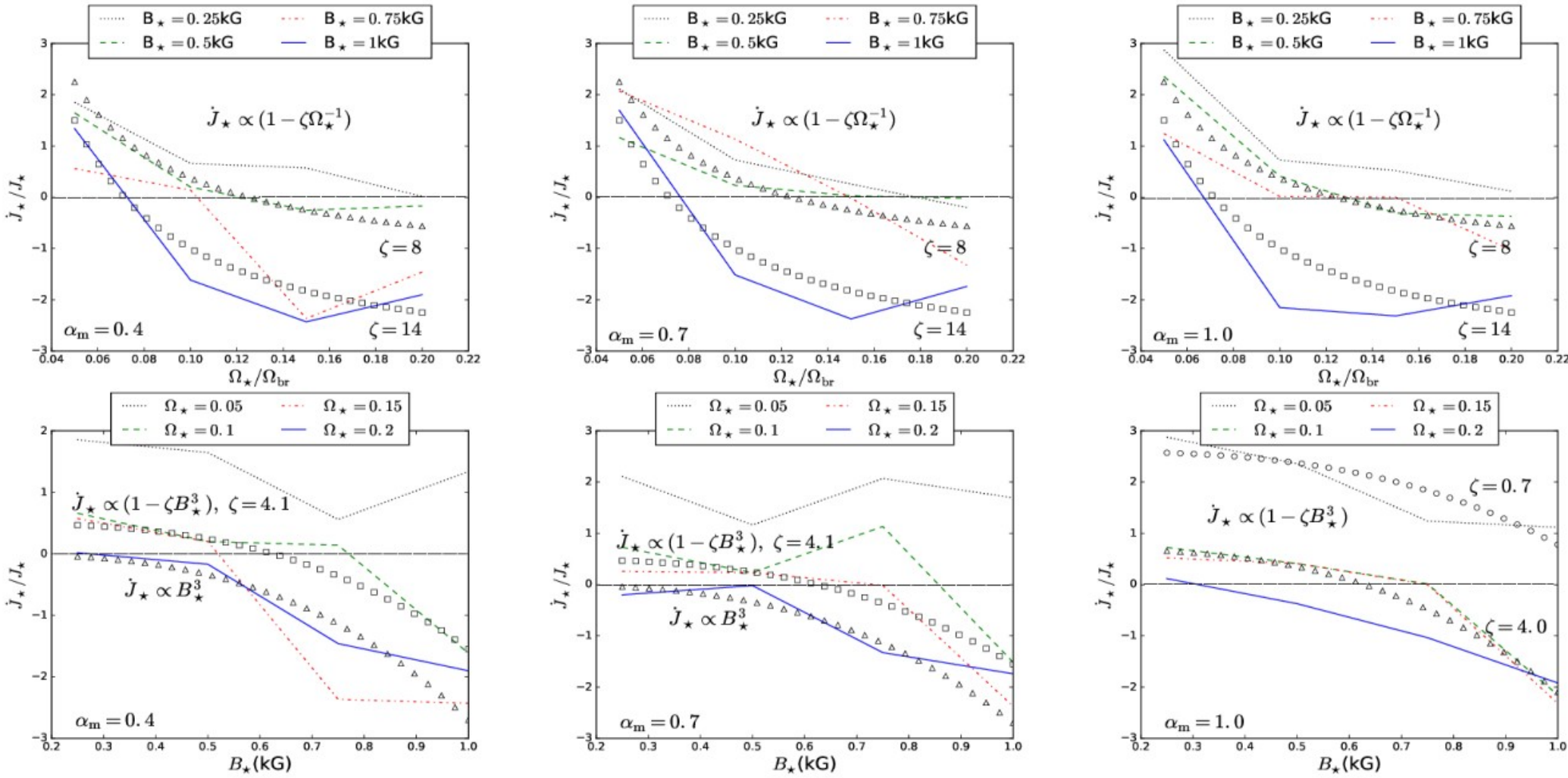

Fig. 7. Torques exerted on the star by material in-falling from the disk in all the cases without conical outflow-this are all the cases except a,b,c,d(1,5,9,13)-with the resistive coefficient $\alpha_{\rm m}$=0.4, 0.7 and 1.0. Approximate matching functions and trends in solutions with different stellar rotation rates and magnetic field strengths are shown as $\dot{J}_\star(\Omega_\star)$ (top panels) and $\dot{J}_\star(B_\star)$ (bottom panels).

Torques with the disk field included in the computation

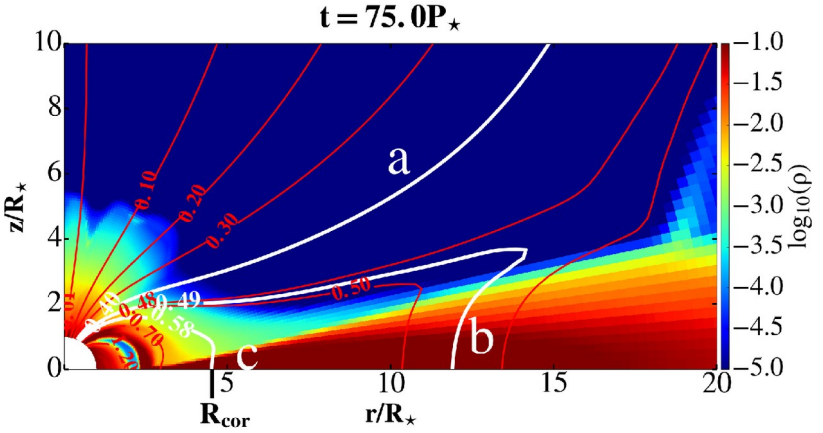

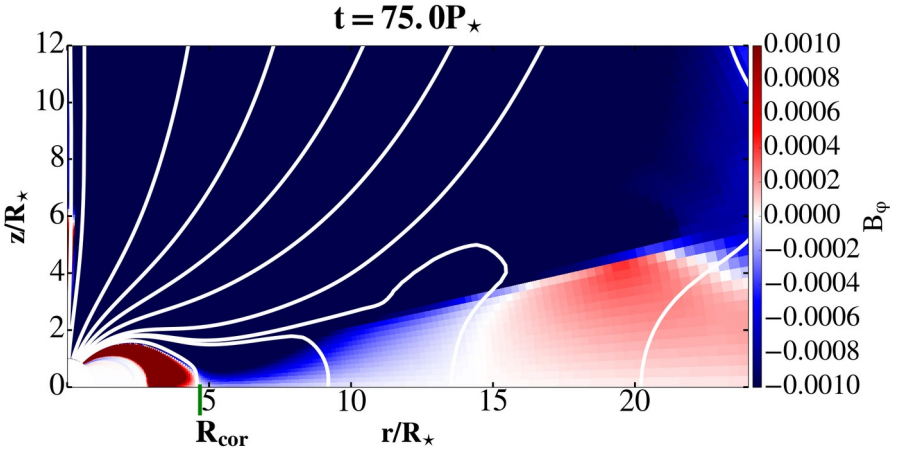

In Naso & Miller (2010, 2011) and Naso et al. (2013) the torques were for the first time computed with the disk field taken into account-in Shakura-Sunyaev (1973) and subsequent computations this is usually neglected. Different vertical zones inside the disk may spin-up or spin-down the central star, regardless of the position of the corotation radius, where the material in the disk corotates with the stellar surface. In the bottom figure we show the difference in the case with 500 G stellar dipole field and both viscous and resistive coefficients equal to unity, in the case with stellar rotation rate 10% of the breakup rate.

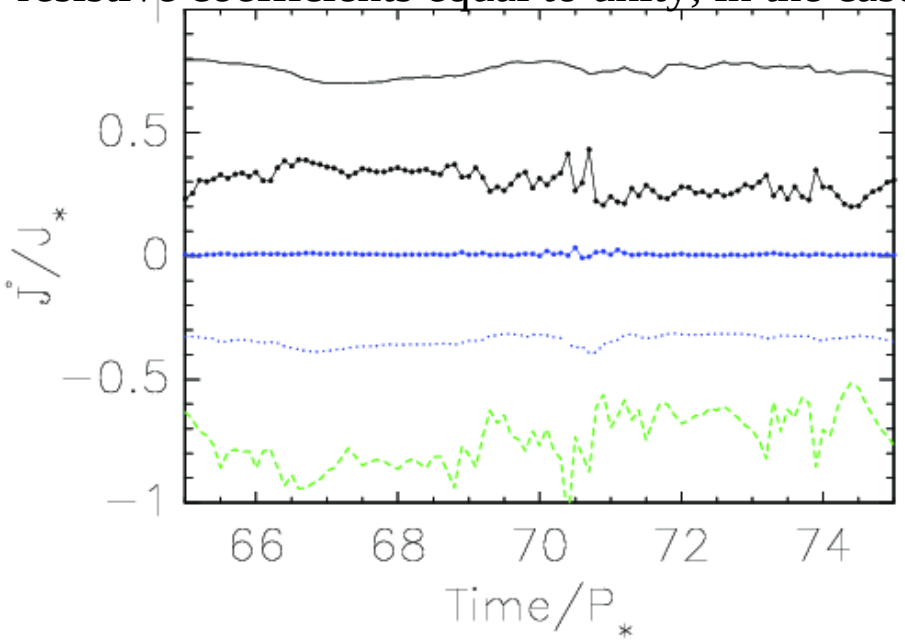

With the dashed (green) line is shown the torque by the stellar (magnetospheric) wind. The torques by the matter flowing onto the star through the accretion column from the distance beyond and below the corotation radius are shown with the dotted (blue) and solid (black) lines, respectively.

With the lines of the same color, but with added thick dots, are shown the torques computed with the inclusion of the magnetic field inside the disk.

Summary

-The purely hydro-dynamic analytical solutions for a thin disk are available in Kluźniak & Kita 2000. We use them as initial state for magnetic simulations.

-We obtained a quasi-stationary state in a set of about 70 viscous and resistive MHD simulations with slowly rotating stars (up to 0.2 of the breakup stellar rotation rate). They are re-scalable to YSOs, WDs and Nss. Results are compared to find trends for angular momentum in the solutions.

-We also computed the torques with the magnetic field inside the disk taken into account. In some cases, this completely changes the outcome!